

Acoustic wave propagation in a porous medium saturated with two fluids and a solid

Lin Liu(刘琳), Xiu-Mei Zhang(张秀梅), and Xiu-Ming Wang(王秀明)

Citation : Chin. Phys. B, 2025, 34 (**2**): 024301. DOI: 10.1088/1674-1056/ad9d17
Journal homepage: http://cpb.iphy.ac.cn; http://iopscience.iop.org/cpb

What follows is a list of articles you may be interested in

Orbital angular momentum conversion of acoustic vortex beams via planar lattice coupling

Qingbang Han(韩庆邦), Zhipeng Liu(刘志鹏), Cheng Yin(殷澄), Simeng Wu(吴思梦), Yinlong Luo(罗寅龙), Zixin Yang(杨子鑫), Xiuyang Pang(庞修洋), Yiqiu Wang(王溢秋), Xuefen Kan(阚雪芬), Yuqiu Zhang(张雨秋), Qiang Yu(俞强), and Jian Wu(吴坚)
Chin. Phys. B, 2024, 33 (**9**): 094301. DOI: 10.1088/1674-1056/ad57ad

Pipeline thickness estimation using the dispersion of higher-order SH guided waves

Zhengchen Dai(代政辰), Jinxia Liu(刘金霞), Yunfei Long(龙云飞), Jianhai Zhang(张建海), Tribikram Kundu, and Zhiwen Cui(崔志文)
Chin. Phys. B, 2024, 33 (**7**): 074301. DOI: 10.1088/1674-1056/ad3033

Experimental realization of fractal fretwork metasurface for sound anomalous modulation

Jiajie He(何佳杰), Shumeng Yu(于书萌), Xue Jiang(江雪), and Dean Ta(他得安)
Chin. Phys. B, 2024, 33 (**5**): 054301. DOI: 10.1088/1674-1056/ad2dcd

Theory of complex-coordinate transformation acoustics for non-Hermitian metamaterials

Hao-Xiang Li(李澔翔), Yang Tan(谭杨), Jing Yang(杨京), and Bin Liang(梁彬)
Chin. Phys. B, 2023, 32 (**9**): 094301. DOI: 10.1088/1674-1056/acc3fc

Theoretical analysis and numerical simulation of acoustic waves in gas hydrate-bearing sediments

Lin Liu(刘琳), Xiu-Mei Zhang(张秀梅), and Xiu-Ming Wang(王秀明)
Chin. Phys. B, 2021, 30 (**2**): 024301. DOI: 10.1088/1674-1056/abcf96

Acoustic wave propagation in a porous medium saturated with two fluids and a solid

Lin Liu(刘琳)[1,3], Xiu-Mei Zhang(张秀梅)[1,2,3,†], and Xiu-Ming Wang(王秀明)[1,2,3]

[1] *State Key Laboratory of Acoustics, Institute of Acoustics, Chinese Academy of Sciences, Beijing* 100190, *China*
[2] *University of Chinese Academy of Sciences, Beijing* 100149, *China*
[3] *Beijing Engineering Research Center of Sea Deep Drilling and Exploration, Institute of Acoustics, Chinese Academy of Sciences, Beijing* 100190, *China*

(Received 8 October 2024; revised manuscript received 28 November 2024; accepted manuscript online 11 December 2024)

Wave propagation in multi-phase porous media is a significant research topic. There are a series of studies about porous media saturated with a single fluid, a solid and a fluid, two fluids, and three fluids. Some gas hydrate-bearing sediments are typical multiphase porous media saturated with a solid (gas hydrates) and two fluids (water and gas). Based on existing theories of porous media, we develop a theory and give a comprehensive analysis of wave propagation in a poroelastic medium saturated with two fluids and a solid. Initially, we establish the constitutive relations and equations of motion. Based on Biot's approach for describing the equations of motion in fluid-saturated porous media at the macroscale, the kinetic energy density, potential energy density, and dissipative energy density are derived. After deriving the equations of motion, a plane wave analysis predicts the existence of four compressional waves, denoted P1, P2, P3, and P4 waves, and two shear waves, denoted S1 and S2 waves. Numerical examples are presented to demonstrate how velocities and attenuations of various waves behave with gas saturation, gas hydrate saturation, and frequency. A model degradation to porous media saturated with a single fluid supports the validity of the theory, which enriches the theory of multiphase porous media and provides a foundation for the evaluation of gas hydrate-bearing sediments.

Keywords: four-phase porous media, equations of motion, plan wave analysis, wave characteristics

PACS: 43.20.+g, 91.60.Lj, 91.30.Cd

DOI: 10.1088/1674-1056/ad9d17 **CSTR:** 32038.14.CPB.ad9d17

1. Introduction

The investigation of acoustic wave propagation in porous media has been a subject of comprehensive research for more than thirty years. Biot's theory[1–4] postulates the presence of two distinct types of compressional waves (including a fast compressional wave and a slow compressional wave) and a shear wave in a fluid-saturated porous medium. The existence of the slow compressional wave is confirmed by Plona,[5] who used an experiment to observe the slow compressional wave at ultrasonic frequencies.

Porous media are often more complex than being simply saturated by a single-phase fluid. Thus, it is essential to develop an acoustic propagation model that incorporates porous media saturated with different solids or fluids. Previous research has extensively explored the propagation of waves in porous media that are saturated with two distinct fluids, employing the equivalent fluid theory to model these complex interactions.[6,7] In these studies, enhanced parameters from liquid–liquid or gas–liquid mixtures are substituted into Biot's theory. However, this model does not account for inertial coupling between fluids, nor between fluids and solids. Considering inertial coupling between different phases and capillary pressure, Santos *et al.*[8,9] introduced a wave propagation theory for porous media saturated with two non-miscible fluids using the virtual complementary work principle. The theory indicates the presence of three compressional waves (including two slow compressional waves) and a singular shear wave in porous media saturated with two fluids. Subsequently, Lo *et al.*[10,11] formulated a model for wave propagation in an elastic porous solid saturated with two non-miscible fluids. Vasco[12] analyzed a porous solid saturated by three fluid phases using a volume-averaging approach. Building on this, Santos[13,14] presented a model to describe the propagation of waves in a poroelastic medium saturated by a three-phase viscous, compressible fluid and described the wave propagation in such a porous medium. For porous media with a solid and a fluid in pores, Leclaire *et al.*[15] introduced a percolation theory built upon Biot's framework, characterizing the acoustic wave propagation in porous media, where a solid grain matrix, ice, and water coexist. However, there is an assumption that the solid frame and ice did not directly contact each other in Leclaire's model. Building on this foundation, Carcione *et al.*[16] advanced the model by incorporating direct contact, and obtained three compressional waves (including two slow compressional waves) and two shear waves (including one slow shear wave) in such a three-phase porous medium. With natural gas hydrates identified as a promising energy source,[17–20] the exploration and development methodologies of gas hy-

†Corresponding author. E-mail: zhangxiumei@mail.ioa.ac.an

© 2025 Chinese Physical Society and IOP Publishing Ltd. All rights, including for text and data mining, AI training, and similar technologies, are reserved.

drates have gained significant research attention.[21–25] Subsequently, due to the similarity in properties between natural gas hydrates and ice, scholars extended the Carcinone–Lalaire model and applied it to natural gas hydrate-bearing sediments, using the velocity and attenuation of mode waves to estimate the saturation of natural gas hydrates.[26–31]

Based on the above work, it's evident that the multiphase porous medium theory plays a pivotal role in the exploration of oil, gas, and natural gas hydrates. However, some gas hydrate-bearing sediments are composed of a solid frame, with gas hydrate, water and gas in pores. There is almost no theory for acoustic wave propagation in porous media containing two fluids and two solids, which is important for the evaluation of natural gas hydrate-bearing sediments. Zhou *et al.*[32] introduced an innovative approach to developing general mechanical equations by using the principle of energy conservation. In the work, for the first time, the elastodynamic equation of motion was derived specifically for porous elastic media that are both arbitrarily anisotropic and multiphasic. However, their work only introduced the process of establishing the equations of motion from another perspective, there is no specific acoustic model in the work that describes the propagation of waves in the model of two types of solids and two kinds of fluids, which has no definition of specific parameters involved, making it impossible to further apply the model to specific analysis.

In this paper, we propose a specific acoustic model for wave propagation in multiphase porous media containing two types of solids and two kinds of fluids at the macroscale. The potential energy density, the stress–strain relations, the kinetic energy density function, and the dissipation energy density function are derived. Next, numerical examples are used to analyze the behavior of all waves as a function of gas saturation, gas hydrate saturation and frequency. Finally, model degradation to a water-saturated porous medium proves the effectiveness of the theoretical model.

2. Potential energy density V

Following Biot's theory, the medium is assumed to exhibit statistical isotropy, characterized by uniform and interconnected porosity ϕ, which is defined as the ratio of the pore volume to the total volume of the medium, as shown in Fig. 1. The solid frame is saturated by two fluids and one solid, taken to be water, gas, and gas hydrate in this paper. The solid frame, water, gas, and gas hydrate are represented by the indices and superindices s, w, g, and h or 1, 2, 3 and 4, respectively. The volumic proportions of the solid frame, water, gas and water, gas and gas hydrate are $\phi_{\rm s}$, $\phi_{\rm w}$, $\phi_{\rm g}$ and $\phi_{\rm h}$, respectively. We assume that the three phases completely saturate the porous, and all phases in the pore are allowed to move within the pore space. There always exists an elementary relationship between the constituent proportions

$$\phi_{\rm s} = 1-\phi, \quad \phi_{\rm w}+\phi_{\rm g}+\phi_{\rm h} = \phi. \tag{1}$$

For arbitrarily anisotropic multiphasic porous media, the potential energy density can be written as[15,32]

$$V = V(e_{ij}^{(\alpha)}), \quad i,j = 1,2,3, \quad \text{and} \quad \alpha = 1,2,\ldots,M, \tag{2}$$

where the elastic strain tensor components are defined as

$$e_{ij}^{(\alpha)} = (u_{i,j}^{(\alpha)} + u_{j,i}^{(\alpha)})/2 \tag{3}$$

in composition α.

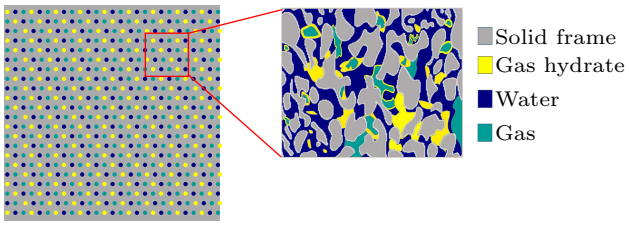


Fig. 1. The schematic model of multiphase porous media saturated with a solid (gas hydrates) and two fluids (water and gas).

In the four-phase case, for small deformations from the equilibrium state, typically associated with elastic waves without external forces, the problem is linearized by expanding V to the second order

$$\begin{aligned} & V\left(e_{ij}^{(1)}, \theta_2, \theta_3, e_{ij}^{(4)}\right) \\ = \; & V(0,0,0,0) + \partial^2 V/(\partial e_{ij}^{(1)} \partial e_{kl}^{(1)}) e_{ij}^{(1)} e_{kl}^{(1)}/2 \\ & + (\partial^2 V/\partial\theta_2^2)\theta_2^2/2 + (\partial^2 V/\partial\theta_3^2)\theta_3^2/2 \\ & + \partial^2 V/(\partial e_{ij}^{(4)} \partial e_{kl}^{(4)}) e_{ij}^{(4)} e_{kl}^{(4)}/2 + \partial^2 V/(\partial e_{ij}^{(1)} \partial\theta_2) e_{ij}^{(1)} \theta_2 \\ & + \partial^2 V/(\partial e_{ij}^{(1)} \partial\theta_3) e_{ij}^{(1)} \theta_3 + \partial^2 V/(\partial e_{ij}^{(1)} \partial e_{kl}^{(4)}) e_{ij}^{(1)} e_{kl}^{(4)} \\ & + \partial^2 V/(\partial\theta_2\partial\theta_3)\theta_2\theta_3 + \partial^2 V/(\partial\theta_2 \partial e_{ij}^{(4)}) \theta_2 e_{ij}^{(4)} \\ & + \partial^2 V/(\partial\theta_3 \partial e_{ij}^{(4)}) \theta_3 e_{ij}^{(4)} + O^3\left(e_{ij}^{(1)}, \theta_2, \theta_3, e_{ij}^{(4)}\right), \end{aligned} \tag{4}$$

where $\theta_2 = e_{ii}^{(2)}$ and $\theta_3 = e_{ii}^{(3)}$.

We establish a fourth-order tensor of elastic coefficients corresponding to the solid frame (index 1) and gas hydrate (index 4), alongside elastic coefficients of water (index 2) and gas (index 3). The non-stiff part of the velocity–stress differential equations can be written in matrix form as

$$\begin{aligned} & C_{ijkl}^{(1)} = \partial^2 V/(\partial e_{ij}^{(1)} \partial e_{kl}^{(1)}), \quad C_{ijkl}^{(4)} = \partial^2 V/(\partial e_{ij}^{(4)} \partial e_{kl}^{(4)}), \\ & K_2 = \partial^2 V/\partial\theta_2^2, \quad K_3 = \partial^2 V/\partial\theta_3^2, \end{aligned} \tag{5}$$

where K_2 and K_3 refer to the effective bulk moduli of the water and gas, respectively. Six crossed terms appear to define two second-order tensors of elastic coupling coefficients:

$$\begin{aligned} & C_{ij}^{\rm sw} = \partial^2 V/(\partial e_{ij}^{(1)} \partial\theta_2), \quad C_{ij}^{\rm sg} = \partial^2 V/(\partial e_{ij}^{(1)} \partial\theta_3), \\ & C_{ij}^{\rm sh} = \partial^2 V/(\partial e_{ij}^{(1)} \partial e_{ij}^{(4)}), \quad C_{ij}^{\rm wg} = \partial^2 V/(\partial\theta_2 \partial\theta_3), \end{aligned}$$

$$C_{ij}^{\rm wh}=\partial^2 V/(\partial\theta_2\partial e_{ij}^{(4)}),\ \ C_{ij}^{\rm gh}=\partial^2 V/(\partial\theta_3\partial e_{ij}^{(4)}). \quad (6)$$

These crossed terms represent, respectively, the exchange of elastic energy between solid and water, solid and gas, solid and hydrate, water and gas, water and hydrate, gas and hydrate.

The energy contributions of solid and gas hydrate are, respectively, given by

$$V_1=C_{ijkl}^{(1)}e_{ij}^{(1)}e_{kl}^{(1)}/2,\ \ V_4=C_{ijkl}^{(4)}e_{ij}^{(4)}e_{kl}^{(4)}/2. \quad (7)$$

The phases are statistically isotropic, $C_{ijkl}^{(1)}$ and $C_{ijkl}^{(4)}$ can be described using two independent coefficients, V_1 and V_4 can be expressed as

$$V_1=K_1\theta_1^2/2+\mu_1 d_1^2,\ \ V_4=K_4\theta_4^2/2+\mu_4 d_4^2, \quad (8)$$

where K_1 and μ_1 are the effective bulk and shear moduli of the solid phase, respectively. Here, d_1, d_4, θ_1 and θ_4 are the invariants of the strain tensor and are called the deviator and the dilatation:

$$\begin{aligned}&d_{ij}^{(m)}d_{ij}^{(m)}=d_m^2,\ \ e_{ij}^{(m)}e_{ij}^{(m)}=e_m^2,\\ &d_{ij}^{(m)}=e_{ij}^{(m)}-\frac{1}{3}\delta_{ij}\theta_m,\ \ \theta_m=e_{ii}^{(m)},\ \ m=1,4.\end{aligned} \quad (9)$$

The potential energy density is given by

$$\begin{aligned}V\ =\ &K_1\theta_1^2/2+\mu_1 d_1^2+K_2\theta_2^2/2+K_3\theta_3^2/2+K_4\theta_4^2/2\\ &+\mu_4 d_4^2+\mu_{14}d_1d_4+C_{12}\theta_1\theta_2+C_{13}\theta_1\theta_3\\ &+C_{14}\theta_1\theta_4+C_{23}\theta_2\theta_3+C_{24}\theta_2\theta_4+C_{34}\theta_3\theta_4,\end{aligned} \quad (10)$$

where C_{12} is the solid–water elastic coupling, C_{13} refers to the solid–gas elastic coupling, C_{14} represents the solid–hydrate elastic coupling, C_{23} is the water–gas elastic coupling, C_{24} is the water–hydrate elastic coupling, C_{34} is the gas–hydrate elastic coupling. K_1, K_2, K_3, and K_4 are the bulk moduli, μ_1, μ_4, and μ_{14} are the shear moduli. The bulk moduli, shear moduli and elastic coupling coefficients are given in Appendix B.

3. The stress–strain relations

For small deformations, the variation of potential energy of a four-phase porous medium is described using a differential form

$$\begin{aligned}{\rm d}V\ =\ &\partial V/\partial e_{ij}^{(1)}\,{\rm d}e_{ij}^{(1)}+\partial V/\partial\theta_2\,{\rm d}\theta_2\\ &+\partial V/\partial\theta_3\,{\rm d}\theta_3+\partial V/\partial e_{ij}^{(4)}\,{\rm d}e_{ij}^{(4)},\end{aligned} \quad (11)$$

thus, following the work of Leclaire *et al.*,[15] V satisfies the conditions which express the stress tensor for each phase:

$$\begin{aligned}&\sigma_{ij}^{(1)}=\partial V/\partial e_{ij}^{(1)},\ \ \sigma^{(2)}=\partial V/\partial\theta_2,\\ &\sigma^{(3)}=\partial V/\partial\theta_3,\ \ \sigma_{ij}^{(4)}=\partial V/\partial e_{ij}^{(4)}.\end{aligned} \quad (12)$$

Using Eqs. (10) and (12), the stress–strain relationships in a two-dimensional case are expressed as

$$\begin{aligned}\sigma_{xx}^{(1)}\ =\ &(K_1+\mu_1)e_{xx}^{(1)}+(K_1-\mu_1)e_{zz}^{(1)}+C_{12}(e_{xx}^{(2)}+e_{zz}^{(2)})\\ &+C_{13}(e_{xx}^{(3)}+e_{zz}^{(3)})+(C_{14}+\mu_{14}/2)e_{xx}^{(4)}\\ &+(C_{14}-\mu_{14}/2)e_{zz}^{(4)},\end{aligned} \quad (13a)$$

$$\begin{aligned}\sigma_{zz}^{(1)}\ =\ &(K_1+\mu_1)e_{zz}^{(1)}+(K_1-\mu_1)e_{xx}^{(1)}+C_{12}(e_{xx}^{(2)}+e_{zz}^{(2)})\\ &+C_{13}(e_{xx}^{(3)}+e_{zz}^{(3)})+(C_{14}+\mu_{14}/2)e_{zz}^{(4)}\\ &+(C_{14}-\mu_{14}/2)e_{xx}^{(4)},\end{aligned} \quad (13b)$$

$$\begin{aligned}\sigma^{(2)}\ =\ &K_2(e_{xx}^{(2)}+e_{zz}^{(2)})+C_{12}(e_{xx}^{(1)}+e_{zz}^{(1)})\\ &+C_{23}(e_{xx}^{(3)}+e_{zz}^{(3)})+C_{24}(e_{xx}^{(4)}+e_{zz}^{(4)}),\end{aligned} \quad (13c)$$

$$\begin{aligned}\sigma^{(3)}\ =\ &K_3(e_{xx}^{(3)}+e_{zz}^{(3)})+C_{13}(e_{xx}^{(1)}+e_{zz}^{(1)})\\ &+C_{23}(e_{xx}^{(2)}+e_{zz}^{(2)})+C_{34}(e_{xx}^{(4)}+e_{zz}^{(4)}),\end{aligned} \quad (13d)$$

$$\begin{aligned}\sigma_{xx}^{(4)}\ =\ &(K_4+\mu_4)e_{xx}^{(4)}+(K_4-\mu_4)e_{zz}^{(4)}+(C_{14}+\frac{1}{2}\mu_{14})e_{xx}^{(1)}\\ &+(C_{14}-\frac{1}{2}\mu_{14})e_{zz}^{(1)}+C_{24}(e_{xx}^{(2)}+e_{zz}^{(2)})\\ &+C_{34}(e_{xx}^{(3)}+e_{zz}^{(3)}),\end{aligned} \quad (13e)$$

$$\begin{aligned}\sigma_{zz}^{(4)}\ =\ &(K_4+\mu_4)e_{zz}^{(4)}+(K_4-\mu_4)e_{xx}^{(4)}+(C_{14}+\frac{1}{2}\mu_{14})e_{zz}^{(1)}\\ &+(C_{14}-\frac{1}{2}\mu_{14})e_{xx}^{(1)}+C_{24}(e_{xx}^{(2)}+e_{zz}^{(2)})\\ &+C_{34}(e_{xx}^{(3)}+e_{zz}^{(3)}),\end{aligned} \quad (13f)$$

$$\sigma_{xz}^{(1)}\ =\ 2\mu_1 e_{xz}^{(1)}+\mu_{14}e_{xz}^{(4)}, \quad (13g)$$

$$\sigma_{xz}^{(4)}\ =\ 2\mu_4 e_{xz}^{(4)}+\mu_{14}e_{xz}^{(1)}. \quad (13h)$$

4. Kinetic energy density T

The kinetic energy density function is similarly structured across each medium component, which has relatively coupled motions between the four components. Thus, the total kinetic energy density for a four-phase porous medium can be written as

$$\begin{aligned}T\ =\ &\frac{1}{2}[\rho_{11}^a\dot{u}_i^{(1)}\dot{u}_i^{(1)}+\rho_{22}^a\dot{u}_i^{(2)}\dot{u}_i^{(2)}+\rho_{33}^a\dot{u}_i^{(3)}\dot{u}_i^{(3)}+\rho_{44}^a\dot{u}_i^{(4)}\dot{u}_i^{(4)}\\ &+\rho_{12}^a(\dot{u}_i^{(1)}-\dot{u}_i^{(2)})(\dot{u}_i^{(1)}-\dot{u}_i^{(2)})\\ &+\rho_{13}^a(\dot{u}_i^{(1)}-\dot{u}_i^{(3)})(\dot{u}_i^{(1)}-\dot{u}_i^{(3)})\\ &+\rho_{14}^a(\dot{u}_i^{(1)}-\dot{u}_i^{(4)})(\dot{u}_i^{(1)}-\dot{u}_i^{(4)})\\ &+\rho_{23}^a(\dot{u}_i^{(2)}-\dot{u}_i^{(3)})(\dot{u}_i^{(2)}-\dot{u}_i^{(3)})\\ &+\rho_{24}^a(\dot{u}_i^{(2)}-\dot{u}_i^{(4)})(\dot{u}_i^{(2)}-\dot{u}_i^{(4)})\\ &+\rho_{34}^a(\dot{u}_i^{(3)}-\dot{u}_i^{(4)})(\dot{u}_i^{(3)}-\dot{u}_i^{(4)})].\end{aligned} \quad (14)$$

Thus, we have

$$\begin{aligned}T\ =\ &(\rho_{11}^a+\rho_{12}^a+\rho_{13}^a+\rho_{14}^a)\dot{u}_i^{(1)}\dot{u}_i^{(1)}\\ &+(\rho_{21}^a+\rho_{22}^a+\rho_{23}^a+\rho_{24}^a)\dot{u}_i^{(2)}\dot{u}_i^{(2)}\\ &+(\rho_{31}^a+\rho_{32}^a+\rho_{33}^a+\rho_{34}^a)\dot{u}_i^{(3)}\dot{u}_i^{(3)}\end{aligned}$$

$$
\begin{aligned}
&+(\rho_{41}^a+\rho_{42}^a+\rho_{43}^a+\rho_{44}^a)\dot{u}_i^{(4)}\dot{u}_i^{(4)}\\
&-2\rho_{12}^a\dot{u}_i^{(1)}\dot{u}_i^{(2)}-2\rho_{13}^a\dot{u}_i^{(1)}\dot{u}_i^{(3)}\\
&-2\rho_{14}^a\dot{u}_i^{(1)}\dot{u}_i^{(4)}-2\rho_{23}^a\dot{u}_i^{(2)}\dot{u}_i^{(3)}\\
&-2\rho_{24}^a\dot{u}_i^{(2)}\dot{u}_i^{(4)}-2\rho_{34}\dot{u}_i^{(3)}\dot{u}_i^{(4)}. \qquad (15)
\end{aligned}
$$

We denote

$$
\begin{aligned}
&\rho_{11}=\rho_{11}^a+\rho_{12}^a+\rho_{13}^a,\ \ \rho_{22}=\rho_{21}^a+\rho_{22}^a+\rho_{23}^a,\\
&\rho_{33}=\rho_{31}^a+\rho_{32}^a+\rho_{33}^a,\ \ \rho_{12}=-\rho_{12}^a,\\
&\rho_{13}=-\rho_{13}^a,\ \ \rho_{14}=-\rho_{14}^a,\ \ \rho_{23}=-\rho_{23}^a,\\
&\rho_{24}=-\rho_{24}^a,\ \ \rho_{34}=-\rho_{34}^a. \qquad (16)
\end{aligned}
$$

The kinetic energy density of a multiphasic porous medium is given by

$$
T=\frac{1}{2}\rho_{\alpha\beta}\dot{u}_i^{(\alpha)}\dot{u}_i^{(\beta)},\ \ i=1,2,3,\ \text{and}\ \ \alpha,\beta=1,2,\ldots,M, \quad (17)
$$

where $\rho_{\alpha\beta}=\rho_{\beta\alpha}$. For our four-phase case, the displacements of solid, water, gas, and hydrate are, respectively, represented by the vectors $u_i^{(1)}$, $u_i^{(2)}$, $u_i^{(3)}$ and $u_i^{(4)}$. The kinetic energy density T is a function of velocities $\dot{u}_i^{(1)}$, $\dot{u}_i^{(2)}$, $\dot{u}_i^{(3)}$ and $\dot{u}_i^{(4)}$ expressed as the time derivative of displacements. Expanding T to the second order and assuming that the motions of the phases are only caused by the wave propagation, we have

$$
\begin{aligned}
T=\ &\frac{1}{2}[\rho_{11}\dot{u}_i^{(1)2}+\rho_{22}\dot{u}_i^{(2)2}+\rho_{33}\dot{u}_i^{(3)2}+\rho_{44}\dot{u}_i^{(4)2}\\
&+2\rho_{12}\dot{u}_i^{(1)}\dot{u}_i^{(2)}+2\rho_{13}\dot{u}_i^{(1)}\dot{u}_i^{(3)}+2\rho_{14}\dot{u}_i^{(1)}\dot{u}_i^{(4)}\\
&+2\rho_{23}\dot{u}_i^{(2)}\dot{u}_i^{(3)}+2\rho_{24}\dot{u}_i^{(2)}\dot{u}_i^{(4)}+2\rho_{34}\dot{u}_i^{(3)}\dot{u}_i^{(4)}], \quad (18)
\end{aligned}
$$

where ρ_{11}, ρ_{22}, ρ_{33}, and ρ_{44} are the mass densities of the effective solid grain, effective water, effective gas and effective gas hydrate, respectively. ρ_{12}, ρ_{13}, ρ_{14}, ρ_{23}, ρ_{24}, ρ_{34} are coupling mass densities caused by relative motion of solid grain and water, solid grain and gas, solid grain and gas hydrate, water and gas, water and gas hydrate, gas and gas hydrate.

Following Biot,[1] Santos[8] and Carcione,[16] the determination of the generalized mass densities ρ_{ij} appearing in Eq. (18) of kinetic energy may be expressed as functions of the combination of the phase proportions, mass densities and parameters that characterize the geometric properties of the solid and hydrate matrices. The generalized mass densities ρ_{ij} are directly extended from the coupling density ρ_{12} in Biot's theory. ρ_{12}, ρ_{13}, ρ_{14}, ρ_{23}, ρ_{24}, ρ_{34} reflect the inertial coupling effect between the phases. In particular, Santos[8] believes that change of ρ_{23} has little impact on velocity and attenuation, so the expression for ρ_{23} is based on experience. The expressions of generalized mass densities ρ_{ij} are given in Appendix C.

5. Dissipation potential D

The dissipative energy density can be written as[15]

$$
\phi_{\mathrm{d}}=\frac{1}{2}b_{\alpha\beta}\dot{w}_i^{(\alpha,\beta)}\dot{w}_i^{(\alpha,\beta)},
$$

$$
i,j=1,2,3,\ \ \text{and}\ \ \alpha=1,2,\ldots,M, \quad (19)
$$

where $\dot{w}_i^{(\alpha,\beta)}=\dot{u}_i^{(\alpha)}-\dot{u}_i^{(\beta)}$ is the relative velocity component between compositions α and β in the i-direction. $b_{\alpha\beta}$ is the friction coefficient,[1] and $b_{\alpha\beta}=b_{\beta\alpha}$. Only dissipations caused by viscous flows are considered.

In our four-phase case, the dissipated energy density is given by a linear function of the velocity differences

$$
\begin{aligned}
D=\ &\frac{1}{2}[b_{12}(\dot{u}_i^{(1)}-\dot{u}_i^{(2)})^2+b_{13}(\dot{u}_i^{(1)}-\dot{u}_i^{(3)})^2\\
&+b_{23}(\dot{u}_i^{(2)}-\dot{u}_i^{(3)})^2+b_{14}(\dot{u}_i^{(1)}-\dot{u}_i^{(4)})^2\\
&+b_{24}(\dot{u}_i^{(2)}-\dot{u}_i^{(4)})^2+b_{34}(\dot{u}_i^{(3)}-\dot{u}_i^{(4)})^2], \quad (20)
\end{aligned}
$$

where b_{12}, b_{13}, b_{14}, b_{23}, b_{24}, b_{34} refer to the friction coefficients between solid grain and water, solid grain and gas, solid grain and gas hydrate, water and gas, water and gas hydrate, gas and gas hydrate, respectively. The expressions of friction coefficients are given in Appendix D.

6. Equations of motion

Lagrange's equation with dissipation potential with displacement as generalized coordinates is given by[15]

$$
\frac{\mathrm{d}}{\mathrm{d}t}\frac{\partial L}{\partial\dot{q}_i^{(m)}}+\left[\frac{\partial L}{\partial\left(q_{i,j}^{(m)}\right)}\right]_{i,j}-\frac{\partial L}{\partial q_i^{(m)}}+\frac{\partial D}{\partial\dot{q}_i^{(m)}}=0. \quad (21)
$$

By substituting kinetic energy density, potential energy density and dissipation potential density into Lagrange's equation, the equations of motion can be obtained as

$$
\begin{aligned}
\sigma_{ij,j}^{(1)}=\ &\rho_{11}\ddot{u}_i^{(1)}+\rho_{12}\ddot{u}_i^{(2)}+\rho_{13}\ddot{u}_i^{(3)}+\rho_{14}\ddot{u}_i^{(4)}\\
&+b_{12}(\dot{u}_i^{(1)}-\dot{u}_i^{(2)})+b_{13}(\dot{u}_i^{(1)}-\dot{u}_i^{(3)})\\
&+b_{14}(\dot{u}_i^{(1)}-\dot{u}_i^{(4)}), \qquad (22a)\\
\sigma_{,i}^{(2)}=\ &\rho_{12}\ddot{u}_i^{(1)}+\rho_{22}\ddot{u}_i^{(2)}+\rho_{23}\ddot{u}_i^{(3)}+\rho_{24}\ddot{u}_i^{(4)}\\
&+b_{12}(\dot{u}_i^{(2)}-\dot{u}_i^{(1)})+b_{23}(\dot{u}_i^{(2)}-\dot{u}_i^{(3)})\\
&+b_{24}(\dot{u}_i^{(2)}-\dot{u}_i^{(4)}), \qquad (22b)\\
\sigma_{ij,j}^{(3)}=\ &\rho_{13}\ddot{u}_i^{(1)}+\rho_{23}\ddot{u}_i^{(2)}+\rho_{33}\ddot{u}_i^{(3)}+\rho_{34}\ddot{u}_i^{(4)}\\
&+b_{13}(\dot{u}_i^{(3)}-\dot{u}_i^{(1)})+b_{23}(\dot{u}_i^{(3)}-\dot{u}_i^{(2)})\\
&+b_{34}(\dot{u}_i^{(3)}-\dot{u}_i^{(4)}), \qquad (22c)\\
\sigma_{,i}^{(4)}=\ &\rho_{14}\ddot{u}_i^{(1)}+\rho_{24}\ddot{u}_i^{(2)}+\rho_{34}\ddot{u}_i^{(3)}+\rho_{44}\ddot{u}_i^{(4)}\\
&+b_{14}(\dot{u}_i^{(4)}-\dot{u}_i^{(1)})+b_{24}(\dot{u}_i^{(4)}-\dot{u}_i^{(2)})\\
&+b_{34}(\dot{u}_i^{(4)}-\dot{u}_i^{(3)}). \qquad (22d)
\end{aligned}
$$

By substituting the constitutive relation into the equations of motion, we can obtain

$$
\tilde{\rho}\ddot{\boldsymbol{u}}+\tilde{b}\dot{\boldsymbol{u}}=\tilde{R}\nabla\nabla\cdot\boldsymbol{u}-\tilde{\mu}\nabla\times\nabla\times\boldsymbol{u}, \quad (23)
$$

where $\tilde{\rho}$, $\tilde{b}$, $\tilde{R}$ and $\tilde{\mu}$ can be expressed as

$$\tilde{\rho}=\begin{pmatrix}\rho_{11}&\rho_{12}&\rho_{13}&\rho_{14}\\ \rho_{12}&\rho_{22}&\rho_{23}&\rho_{24}\\ \rho_{13}&\rho_{23}&\rho_{33}&\rho_{34}\\ \rho_{14}&\rho_{24}&\rho_{34}&\rho_{44}\end{pmatrix},\quad \tilde{R}=\begin{pmatrix}R_{11}&R_{12}&R_{13}&R_{14}\\ R_{12}&R_{22}&R_{23}&R_{24}\\ R_{13}&R_{23}&R_{33}&R_{34}\\ R_{14}&R_{24}&R_{34}&R_{44}\end{pmatrix},\quad \tilde{\mu}=\begin{pmatrix}\mu_{11}&0&\mu_{13}&0\\ 0&0&0&0\\ \mu_{13}&0&\mu_{33}&0\\ 0&0&0&0\end{pmatrix},$$

$$\tilde{b}=\begin{pmatrix}b_{12}+b_{13}+b_{14}&-b_{12}&-b_{13}&-b_{14}\\ -b_{12}&b_{12}+b_{23}+b_{24}&-b_{23}&-b_{24}\\ -b_{13}&-b_{23}&b_{13}+b_{23}+b_{34}&-b_{34}\\ -b_{14}&-b_{24}&-b_{34}&b_{14}+b_{24}+b_{34}\end{pmatrix},$$

where $\boldsymbol{u}=(u_i^{\mathrm{s}},u_i^{\mathrm{w}},u_i^{\mathrm{g}},u_i^{\mathrm{h}})^{\mathrm{T}}$ denotes the displacement matrix. The specific expressions of the matrix of the rigidity moduli are given by

$$\begin{aligned}&R_{11}=K_1+\mu_1,\ \ R_{12}=C_{12},\ \ R_{13}=C_{13},\\ &R_{14}=C_{14}+\frac{1}{2}\mu_{14},\ \ R_{22}=K_{22},\ \ R_{23}=C_{23},\\ &R_{24}=C_{24},\ \ R_{34}=C_{34},\ \ R_{44}=K_4+\mu_4.\end{aligned}$$

7. Plane wave analysis

To derive the governing equations of compressional and shear waves from the equation of motion (Eq. (23)), we apply the divergence and rotational operators

$$\tilde{R}\nabla^2\varphi=\tilde{\rho}\ddot{\varphi}+\tilde{b}\dot{\varphi},\tag{24a}$$

$$\tilde{\mu}\nabla^2\psi=\tilde{\rho}\ddot{\psi}+\tilde{b}\dot{\psi}.\tag{24b}$$

The displacement potentials of compressional and shear waves are given by

$$\begin{pmatrix}\varphi^{\mathrm{s}}\\ \varphi^{\mathrm{w}}\\ \varphi^{\mathrm{g}}\\ \varphi^{\mathrm{h}}\end{pmatrix}=\begin{pmatrix}\boldsymbol{A}_1^{\mathrm{s}}\\ \boldsymbol{A}_1^{\mathrm{w}}\\ \boldsymbol{A}_1^{\mathrm{g}}\\ \boldsymbol{A}_1^{\mathrm{h}}\end{pmatrix}\exp\left(\mathrm{i}\left(k_{\mathrm{P}}\cdot r-\omega t\right)\right),\tag{25a}$$

$$\begin{pmatrix}\psi^{\mathrm{s}}\\ \psi^{\mathrm{w}}\\ \psi^{\mathrm{g}}\\ \psi^{\mathrm{h}}\end{pmatrix}=\begin{pmatrix}\boldsymbol{A}_2^{\mathrm{s}}\\ \boldsymbol{A}_2^{\mathrm{w}}\\ \boldsymbol{A}_2^{\mathrm{g}}\\ \boldsymbol{A}_2^{\mathrm{h}}\end{pmatrix}\exp\left(\mathrm{i}\left(k_{\mathrm{S}}\cdot r-\omega t\right)\right).\tag{25b}$$

By substituting Eqs. (25a) and (25b) into Eqs. (24a) and (24b), the governing equations of compressional and shear waves can be obtained as

$$\left(\omega^2\tilde{\rho}+\mathrm{i}\omega\tilde{b}-k_{\mathrm{P}}^2\tilde{R}\right)\begin{pmatrix}\boldsymbol{A}_1^{\mathrm{s}}\\ \boldsymbol{A}_1^{\mathrm{w}}\\ \boldsymbol{A}_1^{\mathrm{g}}\\ \boldsymbol{A}_1^{\mathrm{h}}\end{pmatrix}=0,\tag{26a}$$

$$\left(\omega^2\tilde{\rho}+\mathrm{i}\omega\tilde{b}-k_{\mathrm{S}}^2\tilde{\mu}\right)\begin{pmatrix}\boldsymbol{A}_2^{\mathrm{s}}\\ \boldsymbol{A}_2^{\mathrm{w}}\\ \boldsymbol{A}_2^{\mathrm{g}}\\ \boldsymbol{A}_2^{\mathrm{h}}\end{pmatrix}=0.\tag{26b}$$

To ensure that the given system of equations has a non-zero solution, the determinant of the coefficient matrix must be zero. By solving the equations, we can obtain four values for k_{P} (compressional wave number) and two values for k_{S} (shear wave number). Therefore, there are four compressional waves and two shear waves in the porous medium consisting of two solids and two fluids.

From the four physical meaningful solutions of the generalized eigenvalue problem Eq. (26a) and two solutions of the generalized eigenvalue problem Eq. (26b), we obtain the phase velocities and inverse quality factors of the waves (P1, P2, P3 and P4 for the four types of compressional waves; S1 and S2 for the two types of shear waves). The velocities can be expressed as

$$V_{\mathrm{P}i}=\frac{\omega}{\mathrm{Re}(k_{\mathrm{P}i})},\ \ i=1,2,3,4,\tag{27a}$$

$$V_{\mathrm{S}i}=\frac{\omega}{\mathrm{Re}(k_{\mathrm{S}i})},\ \ i=1,2.\tag{27b}$$

The inverse quality factor Q^{-1} can be used to evaluate the wave attenuation

$$Q^{-1}=2\mathrm{Im}(k_j)/\mathrm{Re}(k_j),\tag{28}$$

where $j=$ P1, P2, P3, P4, S1 and S2.

8. Numerical examples

We compute the phase velocities and attenuations for a hydrate-bearing sediment saturated by water, gas and gas hydrate. Two typical frequencies are selected: 20 Hz for seismic exploration and 10 kHz for acoustic logging. The saturations of water S_{w}, gas S_{g}, and gas hydrate S_{h} are given by

$$S_{\mathrm{w}}=\frac{\phi_{\mathrm{w}}}{\phi},\ \ S_{\mathrm{g}}=\frac{\phi_{\mathrm{g}}}{\phi},\ \ S_{\mathrm{h}}=\frac{\phi_{\mathrm{h}}}{\phi},\ \ S_{\mathrm{w}}+S_{\mathrm{g}}+S_{\mathrm{h}}=1.\tag{29}$$

The material properties of the hydrate-bearing sediment containing gas are: porosity $\phi=0.3$ and permeability $\kappa_{\mathrm{s}0}=1.07\times10^{-13}$ μm; solid grain density, bulk modulus and shear modulus $\rho_{\mathrm{s}}=2.65$ g/cm^3, $K_{\mathrm{s}}=38.7$ GPa and $G_{\mathrm{s}}=39.6$ GPa, respectively. The permeability of hydrate $\kappa^{\mathrm{h}0}=5\times10^{-4}$ μm; hydrate density, bulk modulus and shear modulus $\rho_{\mathrm{h}}=0.92$ g/cm^3, $K_{\mathrm{h}}=8.58$ GPa and $G_{\mathrm{h}}=3.32$ GPa, respectively. The properties of water and gas in the pore space are: $\rho_{\mathrm{w}}=1$ g/cm^3, $K_{\mathrm{w}}=2.25$ GPa, $\eta_{\mathrm{w}}=1.8\times10^{-3}$ Pa·s, $\rho_{\mathrm{g}}=0.079$ g/cm^3, $K_{\mathrm{g}}=12.7$ MPa, $\eta_{\mathrm{g}}=0.1\times10^{-3}$ Pa·s, respectively. The capillary pressure coefficient B is 3×10^3 Pa.

The residual saturations of the two fluids S_{rw} and S_{rg} are 0.05 and 0, respectively. The absolute reference pressure $\bar{p}_w$ is 30×10^6 Pa.

Figures 2 and 3 show phase velocities of two fast and four slow waves as a function of gas saturation, respectively. The frequencies are (a) 20 Hz and (b) 10 kHz, the porosity ϕ is 0.3, and the gas hydrate saturation S_h is 0.4. Through plane wave analysis, it can be found that there are four compressional waves and two shear waves in porous media containing two solids and two fluids, including three slow compressional and one slow shear waves. This is because the relative motion between the solid frame and gas hydrates produces one slow compressional wave and one slow shear wave, while the relative motion between the solid frame and water (gas) produces two slow compressional waves. It can be observed in Fig. 2 that at the two frequencies, the P1 and S1 velocities display a decreasing behavior with the increase of gas saturation. The velocities of P2, S2, P3 and P4 waves displayed in Fig. 3 are slower than those of the P1 and S1 waves, and the velocities of slow waves are higher at the high frequency (10 kHz) than those at the low frequency (20 Hz). The velocities of the slow waves are minimally affected by the gas saturation.

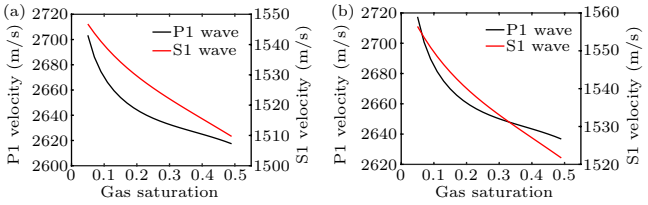


Fig. 2. Phase velocities of P1 and S1 waves as a function of gas saturation. The frequency is (a) 20 Hz and (b) 10 kHz, the porosity $\phi = 0.3$, and the gas hydrate saturation $S_h = 0.4$.

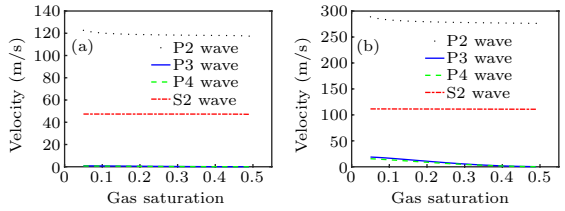


Fig. 3. Phase velocities of four types of slow waves as a function of gas saturation. The slow waves are labeled P2, P3, P4 and S2. The porosity $\phi = 0.3$, and the gas hydrate saturation $S_h = 0.4$. The frequency is (a) 20 Hz and (b) 10 kHz.

Figures 4 and 5 show phase velocities of two fast and four slow waves for the elastic case as a function of gas hydrate saturation, respectively. The frequencies are (a) 20 Hz and (b) 10 kHz, the porosity ϕ is 0.3, and the gas saturation S_n is 0.15. It can be observed in Fig. 4 that the P1 and S1 velocities increase as the gas hydrate saturation increases. The velocities of the P1 and S1 waves are almost unaffected by the frequency, this is the same as the conclusion of other multiphase porous media such as Biot's theory and three-phase theory. The velocities of the four types of slow waves in Fig. 5 exhibit different trends with the gas hydrate saturation at low (20 Hz) and high (10 kHz) frequencies.

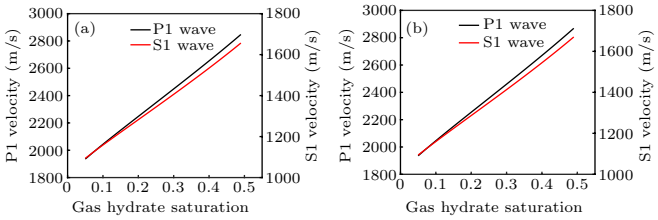


Fig. 4. Phase velocities of P1 and S1 waves as a function of gas hydrate saturation. The porosity $\phi = 0.3$, and the gas hydrate saturation $S_g = 0.15$. The frequency is (a) 20 Hz and (b) 10 kHz.

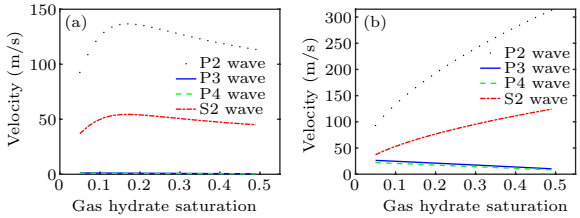


Fig. 5. Phase velocities of four types of slow waves as a function of gas saturation. The slow waves are labeled P2, P3, P4 and S2. The porosity $\phi = 0.3$, and the gas hydrate saturation $S_g = 0.15$. The frequency is (a) 20 Hz and (b) 10 kHz.

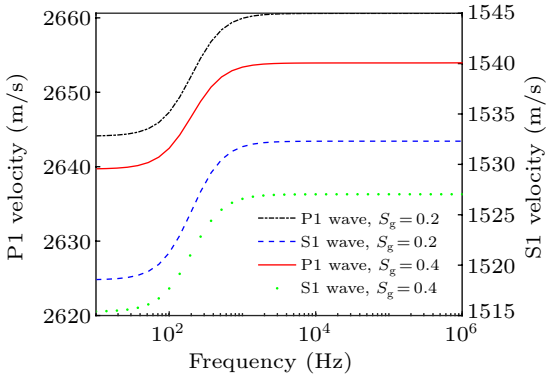


Fig. 6. Phase velocities of P1 and S1 waves as a function of frequency. The porosity $\phi = 0.3$, the gas hydrate saturation $S_h = 0.4$, and the gas saturation $S_g = 0.2$ and 0.4, respectively.

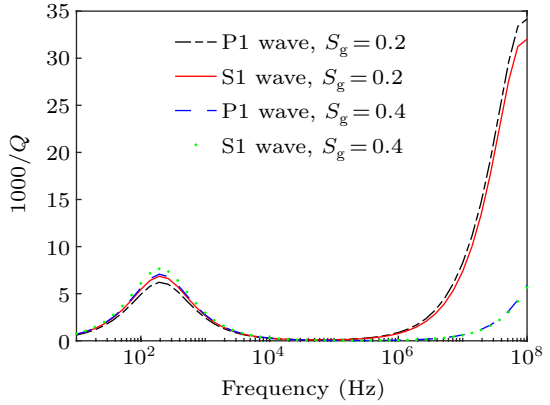


Fig. 7. Attenuations of P1 and S1 waves as a function of frequency. The porosity $\phi = 0.3$, the gas hydrate saturation $S_h = 0.4$, and the gas saturation $S_g = 0.2$ and 0.4, respectively.

Figures 6 and 7 show phase velocities and attenuations of P1 and S1 waves as a function of frequency, respectively. The

porosity ϕ is 0.3, gas hydrate saturation S_h is 0.4, and the gas saturations S_g are 0.2 and 0.4, respectively. It can be observed that P1 and S1 waves exhibit rapid propagation, comparable to P and S waves in a single-phase elastic medium. Furthermore, P1 and S1 waves show minimal dispersion within the frequency ranges of seismic exploration (10 Hz–100 Hz) and acoustic logging (1 kHz–20 kHz). Notice that there are dispersion transition bands of P1 and S1 waves in the frequency range of 100 Hz–1 kHz. These characteristics are similar to those in the three-phase porous media we have analyzed in the previous research.[33] For attenuation, as can be observed in Fig. 7 (expanding attenuation by 1000 times), the attenuations of these two waves exhibit minimal values, although they both have peaks in attenuation. Initially, their attenuations increase, then decrease, and subsequently may decrease again as frequency increases. It can be observed in Fig. 7 that there are two obvious attenuation peaks of P1 and S1 waves, this is due to the two solids in the porous media.

Previous research has shown that the attenuation characteristics of acoustic waves can be used for estimating reservoir characteristics. Figures 8 and 9 show phase velocities and attenuations of four slow waves as functions of frequency. The porosity ϕ is 0.3, the gas hydrate saturation S_h is chosen to be 0.4, and the gas saturation S_g is 0.2. Figure 8 indicates that the velocities of the P2 and S2 waves show a trend of increasing first and then flattening out with increasing frequency. The two slow waves exhibit dispersion in the low-frequency range, whereas there is minimal dispersion observed in the high-frequency range. At low frequencies, P2, S2, P3, and P4 waves propagate slowly primarily due to the significant influence of pore fluid viscosity on velocity. In contrast, at higher frequencies, inertial forces exert a greater impact on wave propagation characteristics. For attenuation, it can be observed in Fig. 9 that the attenuations of the P2 and S2 waves show a trend of first decreasing and then remaining unchanged with increasing frequency. The attenuations of the P3 and P4 waves show a trend of first remaining unchanged and then changing slightly with increasing frequency. Moreover, compared with Fig. 9, the attenuations of the four slow waves are significantly higher, by several orders of magnitude, compared to the attenuations of P1 and S1. Because of their slow propagation velocities and high attenuations in a low frequency band, the four slow waves are challenging to observe, resembling the behavior of slow waves in Biot two-phase media. However, these slow waves do carry some energy but decay rapidly. Scholars still study slow waves because they also carry energy and have a certain impact on the attenuation mechanism. Many scholars have analyzed the slow wave modes propagating in different types of porous media.[34–38] When encountering interfaces, waves also undergo mode conversion. In addition, for acoustic logging, the amplitudes of guided waves received by receivers in a borehole surrounded by different types of porous media are also different, the presence of slow waves can have an impact on the attenuation mechanism of the wavefield, which can be used to estimate the characteristic of the reservoir.[39,40] Therefore, it's important to take into account the impact of slow waves on attenuation.

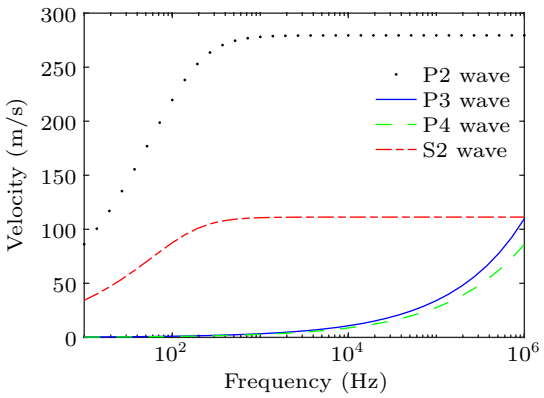


Fig. 8. Phase velocities of four types of slow waves as a function of frequency. The slow waves are labeled P2, P3, P4 and S2. The porosity $\phi = 0.3$, the gas hydrate saturation $S_h = 0.4$, and the gas saturation $S_g = 0.2$.

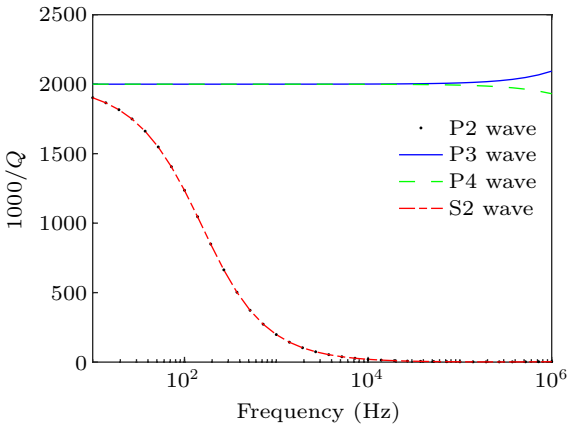


Fig. 9. Attenuations of four types of slow waves as a function of frequency. The porosity $\phi = 0.3$, the gas hydrate saturation $S_h = 0.4$, and the gas saturation $S_g = 0.2$ and 0.4, respectively.

Gas hydrate saturation is an important parameter for hydrate exploration and development. The above research indicates that the velocities and attenuations of P1 and S1 waves are greatly influenced by hydrate saturation and gas saturation. Therefore, the propagation characteristics of the waves can be used to estimate the gas hydrate saturation in hydrate exploration to evaluate hydrate reservoirs.

9. Model degradation

Suppose the pore solid and the gas are completely replaced by water, i.e., $\phi_h = \phi_g = 0$, $\phi_w = \phi$. Therefore, we obtain

$$C_{14} = C_{24} = C_{13} = C_{34} = 0, \quad \gamma = 1, \quad \alpha' = 1, \quad K_f = K_w,$$
$$c_4 = 0, \quad g_4 = 0, \quad K_{hm} = 0,$$

$$K_{\rm av} = [(1-c_1)\phi_{\rm s}/K_{\rm s} + \phi_{\rm w}/K_{\rm w}]^{-1},$$
$$K_3 = K_4 = 0,\ \ \mu_{\rm hm} = 0,\ \ \mu_4 = \mu_{14} = 0,$$
$$\mu_{\rm av} = [(1-g_1)\,\phi_{\rm s}/\mu_{\rm s} + \phi_{\rm w}/({\rm i}\omega\eta_{\rm w})]^{-1},$$
$$A = K_{\rm c}\vartheta,\ \ p_{\rm ca} \to \infty,\ \ p'_{\rm ca} \to \infty,$$
$$\xi = 0,\ \ C_{23} = -A(1/K_{\rm sm}\delta + r/q) = 0.$$

Thus, the stress–strain relations can be expressed as

$$\sigma_{xx}^{(1)} = (K_1+\mu_1)\,e_{xx}^{(1)} + (K_1-\mu_1)\,e_{zz}^{(1)} + C_{12}\left(e_{xx}^{(2)} + e_{zz}^{(2)}\right), \tag{30a}$$
$$\sigma_{zz}^{(1)} = (K_1+\mu_1)\,e_{zz}^{(1)} + (K_1-\mu_1)\,e_{xx}^{(1)} + C_{12}\left(e_{xx}^{(2)} + e_{zz}^{(2)}\right), \tag{30b}$$
$$\sigma^{(2)} = K_2\left(e_{xx}^{(2)} + e_{zz}^{(2)}\right) + C_{12}\left(e_{xx}^{(1)} + e_{zz}^{(1)}\right), \tag{30c}$$
$$\sigma_{xz}^{(1)} = 2\mu_1 e_{xz}^{(1)}. \tag{30d}$$

The stress–strain relations in Biot's theory can be written as

$$\sigma_{xx} = (2N+A)e_{xx} + Ae_{zz} + Q\,(\varepsilon_{xx}+\varepsilon_{zz}), \tag{31a}$$
$$\sigma_{zz} = (2N+A)e_{zz} + Ae_{xx} + Q\,(\varepsilon_{xx}+\varepsilon_{zz}), \tag{31b}$$
$$S = Q\,(e_{xx}+e_{zz}) + R\,(\varepsilon_{xx}+\varepsilon_{zz}), \tag{31c}$$
$$\sigma_{xz} = 2Ne_{xz}, \tag{31d}$$

where σ_{xx} and σ_{zz} refer to the stress of the solid frame in the x direction and z direction, S defines the stress of the pore fluid, A, N, Q and R are elastic parameters. It can be demonstrated that the stress–strain relations of a four-phase porous medium can be simplified to those of a fluid-saturated porous medium through a proof:

$$\mu_1 = N,\ \ K_1 = A+N,\ \ C_{12} = Q,\ \ R = K_2. \tag{32}$$

Here, μ_1 and N refer to the shear modulus, thus we can obtain

$$\mu_1 = N. \tag{33}$$

In Biot's theory, there are

$$A = \lambda + M(\phi-\alpha)^2,\ \ R = \phi^2 M,$$
$$Q = \phi M(\alpha-\phi) = \phi M\,(1-K_{\rm b}/K_{\rm s}-\phi), \tag{34}$$

where

$$\alpha = 1 - K_{\rm b}/K_{\rm s}, \tag{35a}$$
$$\lambda = K_{\rm b} - N, \tag{35b}$$
$$M = (\phi/K_{\rm f} + (\alpha-\phi)/K_{\rm s})^{-1} = (\phi/K_{\rm f} + (\phi_{\rm s} - K_{\rm b}/K_{\rm s})/K_{\rm s})^{-1}. \tag{35c}$$

After degradation, the average bulk modulus can be expressed as

$$K_{\rm av} = [(1-c_1)\,\phi_{\rm s}/K_{\rm s} + \phi/K_{\rm w}]^{-1} = [(\phi_{\rm s} - K_{\rm sm}/K_{\rm s})/K_{\rm s} + \phi/K_{\rm f}]^{-1}. \tag{36}$$

Comparing Eqs. (35c) and (36), we obtain the equivalent relation

$$K_{\rm av} = M. \tag{37}$$

In addition, $K_{\rm sm}$ and $K_{\rm b}$ refer to the elastic modulus of the solid frame, thus, $K_{\rm sm} = K_{\rm b}$. The elastic coupling coefficient of the grain and fluid C_{12} is given by

$$C_{12} = (1-c_1)\,\phi_{\rm s}\phi_{\rm w}K_{\rm av} = (1-\phi-K_{\rm sm}/K_{\rm s})\,\phi M = Q. \tag{38}$$

The bulk modulus of the solid frame K_1 is

$$K_1 = [(1-c_1)\,\phi_{\rm s}]^2 K_{\rm av} + K_{\rm sm} = (\phi_{\rm s} - K_{\rm sm}/K_{\rm s})^2 M + K_{\rm sm} = A + N. \tag{39}$$

Therefore, we can establish the validity of Eq. (32), confirming the validity of our deduction. Additionally, assuming the complete replacement of the pore solid by the fluid suggests that

$$b_{13} = b_{23} = 0,\ \ \rho_{13} = \rho_{23} = \rho_{33} = 0,$$
$$a_{13} = a_{23} = 1,\ \ a_{12} = r_{12}(1-\phi)/\phi + 1. \tag{40}$$

Therefore, the equations of motion can be written as

$$\sigma_{ij,j}^{(1)} = \rho_{11}\dot{v}_i^{(1)} + \rho_{12}\dot{v}_i^{(2)} - b_{12}(v_i^{(2)} - v_i^{(1)}), \tag{41a}$$
$$\sigma_{ij,i}^{(2)} = \rho_{12}\dot{v}_i^{(1)} + \rho_{22}\dot{v}_i^{(2)} + b_{12}(v_i^{(2)} - v_i^{(1)}), \tag{41b}$$

where the mass densities are the same as those in Biot's theory, which are given by

$$\rho_{11} = \phi_{\rm s}\rho_{\rm s} + (a_{12}-1)\phi\rho_{\rm w} = \phi_{\rm s}\rho_{\rm s} + r_{12}\phi_{\rm s}\rho_{\rm f},$$
$$\rho_{22} = a_{12}\phi\rho_{\rm w} = r_{12}\phi_{\rm s}\rho_{\rm f} + \phi\rho_{\rm f},$$
$$\rho_{12} = -(a_{12}-1)\phi\rho_{\rm w} = -r_{12}\phi_{\rm s}\rho_{\rm f}. \tag{42}$$

Therefore, the theory of two solid and two flow porous media can be degenerated into Biot's theory, which to some extent proves the effectiveness of the theory.

10. Conclusion

In this paper, we present a model to describe the propagation of waves in a poroelastic four-phase medium containing two solids and two fluids, showing the existence of four compressional waves (P1, P2, P3 and P4) and two shear waves (S1 and S2). The P1, S1, P2, S2 and P4 waves are analogs of those in the Carcione–Leclaire three-phase theory, while the P3 wave is an additional compressional wave that arises due to the presence of capillary forces between the two fluids.

We compute velocities and attenuations for all these waves as functions of gas saturation, gas hydrate saturation

and frequency. The results indicate that P1 and P2 waves are greatly affected by the gas saturation and gas hydrate saturation. Our research provides a theoretical foundation for practical engineering applications such as the evaluation of gas hydrate reservoirs. We assume an equant-porosity case, we do not consider other complex situations. To better apply theory to practice, more complex structures that fit the actual situation need to be considered in a subsequent study.

Appendix A: List of symbols

b_{12} friction coefficient between the solid grain frame and pore water.

b_{13} friction coefficient between the solid grain frame and gas.

b_{14} friction coefficient between the solid grain frame and gas hydrate.

b_{23} friction coefficient between the pore water and gas.

b_{24} friction coefficient between the pore water and gas hydrate.

b_{34} friction coefficient between the gas and gas hydrate.

ϕ_s volume fraction of solid grain.

ϕ_w volume fraction of pore water.

ϕ_g volume fraction of pore gas.

ϕ_h volume fraction of gas hydrate.

ρ_s solid grain density.

ρ_w water density.

ρ_g water density.

ρ_h gas hydrate density.

κ_{s0} permeability of solid–grain frame.

κ^{h0} permeability of gas–hydrate frame.

K_s solid grain bulk modulus.

K_w water bulk modulus.

K_g gas bulk modulus.

K_h gas hydrate bulk modulus.

μ_s solid grain shear modulus.

μ_h gas hydrate shear modulus.

ρ_{11} effective mass density of solid grain.

ρ_{22} effective mass density of pore water.

ρ_{33} effective mass density of pore gas.

ρ_{44} effective mass density of gas hydrate.

ρ_{12} additional mass density related to the relative motion of solid grain and pore water.

ρ_{13} additional mass density related to the relative motion of solid grain and pore gas.

ρ_{14} additional mass density related to the relative motion of solid grain and gas hydrate.

ρ_{23} additional mass density related to the relative motion of water and gas.

ρ_{24} additional mass density related to the relative motion of water and gas hydrate.

ρ_{34} additional mass density related to the relative motion of gas and gas hydrate.

a_{12} tortuosity for water flowing through the solid grain frame.

a_{13} tortuosity for gas flowing through the solid grain frame.

a_{14} tortuosity for solid grain flowing through the gas hydrate.

a_{23} tortuosity for water flowing through the gas.

a_{24} tortuosity for water flowing through the gas hydrate.

a_{32} tortuosity for gas flowing through the water.

a_{34} tortuosity for gas flowing through the gas hydrate.

a_{41} tortuosity for gas hydrate flowing through the solid grain.

c_1 and g_1 consolidation coefficient for the solid grain.

c_4 and g_4 consolidation coefficient for the gas hydrate.

K_{sm} solid–grain frame bulk modulus.

μ_{sm} solid–grain frame shear modulus.

K_{hm} solid–grain frame bulk modulus.

μ_{hm} solid–grain frame shear modulus.

K_{av} average bulk modulus.

μ_{av} average shear modulus.

C_{12} the solid–water elastic coupling.

C_{13} the solid–gas elastic coupling.

C_{14} the solid–hydrate elastic coupling.

C_{24} the water–hydrate elastic coupling.

C_{34} the gas–hydrate elastic coupling.

Appendix B: Expressions of bulk moduli, shear moduli and elastic coupling coefficients

The K_1, K_2, K_3, and K_4 a are the bulk moduli, according to Leclaire[15] and Carcione and Seriani's[16] work, which can be expressed as

$$K_1 = [(1-c_1)\phi_s]^2 K_{av} + K_{sm},\ \ K_2 = \phi_w^2 K_{av},$$
$$K_3 = \phi_g^2 K_{av},\ \ K_4 = [(1-c_4)\phi_h]^2 K_{av} + K_{hm}. \quad \text{(B1)}$$

μ_1, μ_4, and μ_{14} are the shear moduli (2001), which are given by

$$\mu_1 = [(1-g_1)\phi_s]^2 \mu_{av},\ \ \mu_4 = [(1-g_4)\phi_h]^2 \mu_{av},$$
$$\mu_{14} = (1-g_1)(1-g_4)\phi_s\phi_h\mu_{av}. \quad \text{(B2)}$$

K_{av} is the average bulk modulus defined by

$$K_{av} = \left[\frac{(1-c_1)\phi_s}{K_s} + \frac{\phi_1}{K_f} + \frac{(1-c_4)\phi_h}{K_h}\right]^{-1}, \quad \text{(B3)}$$

μ_{av} is the average shear modulus defined by

$$\mu_{av} = \left[\frac{(1-g_1)\phi_s}{\mu_s} + \frac{\phi_w}{i\omega\eta_w} + \frac{\phi_g}{i\omega\eta_g} + \frac{(1-g_4)\phi_h}{\mu_h}\right]^{-1}, \quad \text{(B4)}$$

K_f represents the bulk modulus of the pore fluid, which was defined in Santos' description of the acoustic propagation model in unsaturated porous media, which can be expressed as $K_f = \alpha'(\frac{\gamma S'_g}{K_g} + \frac{S'_w}{K_w})^{-1}$, and $\gamma = \frac{1+p'_{ca}S'_wS'_g/K_w}{1+p'_{ca}S'_wS'_g/K_g}$, $\alpha' = 1+(\gamma-$

$1)(S'_g+\beta)$, $\phi_1=\phi_w+\phi_g$, $S'_g=\frac{\phi_g}{\phi_1}$, $S'_w=\frac{\phi_w}{\phi_1}$, $\beta=\frac{p_{ca}}{p'_{ca}}$. p_{ca} is the capillary pressure expressed as

$$p_{ca}=B[(S'_g+S_{rw}-1)^{-2}-(S_{rg}/S'_g)^2(1-S_{rg}-S_{rw})^{-2}], \quad \text{(B5)}$$

p'_{ca} is the derivative of capillary pressure p_{ca} with respect to S'_g, B is the capillary pressure coefficient. c_1, c_3, g_1, and g_3 are the consolidation coefficients of solid grain and gas hydrate defined according to the Biot's theory:[1]

$$\begin{aligned} &c_1=K_{sm}/(\phi_s K_s), \quad g_1=\mu_{sm}/(\phi_s\mu_s),\\ &c_4=K_{hm}/(\phi_h K_h), \quad g_4=\mu_{hm}/(\phi_h\mu_h). \end{aligned} \quad \text{(B6)}$$

K_s, K_g, and K_w and K_h are the bulk moduli of solid grain, non-wet phase fluid, wet phase fluid and gas hydrate, respectively. K_{sm} and K_{hm} are the elastic and shear moduli of the solid grain frame and gas hydrate frame. Lee *et al.*[26] express them as

$$\begin{aligned} K_{hm}&=\frac{K_h(1-\phi_{ah})}{(1+\alpha\phi_{ah})}, \quad \mu_{hm}=\frac{\mu_h(1-\phi_{ah})}{(1+\gamma_0\alpha\phi_{ah})},\\ K_{sm}&=\frac{K_s(1-\phi_{as})}{(1+\alpha\phi_{as})}, \quad \mu_{sm}=\frac{\mu_s(1-\phi_{as})}{(1+\gamma_0\alpha\phi_{as})}, \end{aligned} \quad \text{(B7)}$$

where ϕ_{ah} and ϕ_{as} denote the apparent porosities, $\phi_{ah}=1-\phi_h$, $\phi_{as}=\phi_w+\phi_g+\varepsilon\phi_h$, with $\gamma=(1+2\alpha)/(1+\alpha)$. ε and α refer to the free parameters. ε accounts for the support of hydrate to the frame. If ε is taken as 0, it implies the hydrate is completely in the form of solid frame, and if 1 is taken, it indicates the hydrate is completely suspended in the pores. ε has little influence on the calculation results and we take $\varepsilon=0.12$, which was suggested by previous studies. The consolidation coefficient α indicates the cementation of the whole frame, which is a sediment-dependent parameter varying based on the properties of the gas hydrate reservoir, and has a certain effect on the theoretical calculation velocity. α can be calculated using the formula presented by Zhang[28]

$$\alpha=\frac{\mu_{sm}-\rho V_S^2}{2\rho V_S^2}\left(\frac{1}{\phi+(\varepsilon-1)S_h\phi}-1\right),$$

where ρ denotes the density of the porous medium which is given by

$$\rho=\rho_s\phi_s+\rho_w\phi_w+\rho_g\phi_g+\rho_h\phi_h, \quad \text{(B8)}$$

C_{12}, C_{13}, C_{14}, C_{23}, C_{24}, C_{34} in Eqs. (13a)–(13f) are the coupling coefficients of effective solid (1), effective water (2), effective gas (3), and effective hydrate (4). For a three-phase porous medium (without gas), the coupling coefficients C_{12}, C_{14}, C_{24}, were defined by Leclaire,[15] which can be expressed as

$$\begin{aligned} &C_{12}=(1-c_1)\phi_s\phi_w K_{av}, \quad C_{14}=(1-c_1)(1-c_4)\phi_s\phi_h K_{av},\\ &C_{24}=(1-c_4)\phi_w\phi_h K_{av}. \end{aligned} \quad \text{(B9)}$$

Similar to C_{12}, the coupling coefficient between solid grain and gas can be expressed as

$$C_{13}=(1-c_1)\phi_s\phi_g K_{av}, \quad \text{(B10)}$$

the coupling coefficient between gas and gas hydrate can be expressed by

$$C_{34}=(1-c_4)\phi_g\phi_h K_{av}. \quad \text{(B11)}$$

Santos and Savioli[14] defined the coupling coefficient between gas and gas hydrate, considering the influence of capillary force generated by the presence of two immiscible fluids, which can be expressed as

$$C_{23}=-A\left(\frac{1}{K_{sm}\delta}+\frac{r}{q}\right)-\frac{\xi}{q}, \quad \text{(B12)}$$

where

$$\begin{aligned} A&=K_c\vartheta[S'_w+(1-\gamma)\xi],\\ r&=\frac{1}{K_c-K_{sm}}[qA-(S'_g+\beta)K_{sm}\delta],\\ \delta&=\frac{1}{K_s}-\frac{1}{K_{sm}}, \quad \beta=\frac{p_{ca}}{p'_{ca}}, \quad \xi=\frac{\bar{p}_w}{p'_{ca}},\\ q&=\phi_1\left(\frac{1}{K_g}+\frac{1}{p'_{ca}S'_wS'_g}\right),\\ \vartheta&=\frac{1/K_s-1/K_{sm}+\phi(1/K_{sm}-1/K_c)}{\alpha'[1/K_s-1/K_{sm}+\phi(1/K_{sm}-1/K_f)]}, \end{aligned} \quad \text{(B13)}$$

where $\bar{p}_w$ is the absolute reference pressure, S_{rg} and S_{rw} are the residual saturation of the two fluids, respectively. K_c is the bulk modulus of the saturated media,

$$C_{23}=-A\left(\frac{1}{K_{sm}\delta}+\frac{r}{q}\right)-\frac{\xi}{q}, \quad \text{(B14)}$$

Appendix C: Expressions of mass densities

$$\begin{aligned} \rho_{11}&=\phi_s\rho_s a_{14}+(a_{21}-1)\phi_w\rho_w\\ &\quad+(a_{31}-1)\phi_g\rho_g+(a_{41}-1)\phi_h\rho_h, && \text{(C1a)}\\ \rho_{12}&=-(a_{21}-1)\phi_w\rho_w, && \text{(C1b)}\\ \rho_{13}&=-(a_{31}-1)\phi_g\rho_g, && \text{(C1c)}\\ \rho_{14}&=-(a_{14}-1)\phi_s\rho_s-(a_{41}-1)\phi_h\rho_h, && \text{(C1d)}\\ \rho_{22}&=(a_{21}+a_{23}+a_{24}-1)\phi_w\rho_w, && \text{(C1e)}\\ \rho_{33}&=(a_{13}+a_{32}+a_{34}-1)\phi_g\rho_g, && \text{(C1f)}\\ \rho_{23}&=0.1\sqrt{\rho_{22}\rho_{33}}, && \text{(C1g)}\\ \rho_{24}&=-(a_{24}-1)\phi_w\rho_w, && \text{(C1h)}\\ \rho_{44}&=\phi_h\rho_h a_{41}+(a_{24}-1)\phi_w\rho_w\\ &\quad+(a_{14}-1)\phi_s\rho_s+(a_{34}-1)\phi_g\rho_g, && \text{(C1i)}\\ \rho_{34}&=-(a_{34}-1)\phi_g\rho_g. && \text{(C1j)} \end{aligned}$$

According to Santos and Savioli,[14] the tortuosity parameters a_{12}, a_{14}, a_{24}, and a_{41} can be expressed as

$$a_{12}=\frac{\phi_s\rho}{\phi_f\rho_f}r_{12}+1, \quad a_{24}=\frac{\phi_h\rho'}{\phi_f\rho_f}r_{24}+1,$$

$$a_{14}=\frac{\phi_{\rm h}\rho''}{\phi_{\rm s}\rho_{\rm s}}r_{14}+1,\ \ a_{41}=\frac{\phi_{\rm s}\rho''}{\phi_{\rm h}\rho_{\rm h}}r_{41}+1, \tag{C2}$$

where

$$\rho=\frac{\phi_{\rm w}\rho_{\rm w}+\phi_{\rm h}\rho_{\rm h}}{\phi_{\rm w}+\phi_{\rm h}},\ \ \rho'=\frac{\phi_{\rm w}\rho_{\rm w}+\phi_{\rm s}\rho_{\rm s}}{\phi_{\rm w}+\phi_{\rm s}},$$
$$\rho''=\frac{\phi_{\rm h}\rho_{\rm h}+\phi_{\rm s}\rho_{\rm s}}{\phi_{\rm h}+\phi_{\rm s}},\ \ r_{ij}=0.5,\ \ i,j=1,2,3,4. \tag{C3}$$

In Eqs. (C1e) and (C1f), the expressions of effective mass densities of the water ρ_{22} and gas ρ_{33} in pores are related to the parameters a_{13}, a_{23}, a_{32} and a_{34}, we express these tortuosity parameters as

$$a_{13}=\frac{\phi_{\rm s}\rho_1}{\phi_{\rm g}\rho_{\rm g}}r_{13}+1,\ \ a_{34}=\frac{\phi_{\rm h}\rho_1'}{\phi_{\rm g}\rho_{\rm g}}r_{34}+1,$$
$$a_{23}=\frac{\phi_{\rm g}\rho_1''}{\phi_{\rm w}\rho_{\rm w}}r_{23}+1,\ \ a_{32}=\frac{\phi_{\rm w}\rho_1''}{\phi_{\rm g}\rho_{\rm g}}r_{32}+1, \tag{C4}$$

where

$$\rho_1=\frac{\phi_{\rm g}\rho_{\rm g}+\phi_{\rm h}\rho_{\rm h}}{\phi_{\rm g}+\phi_{\rm h}},\ \ \rho_1'=\frac{\phi_{\rm g}\rho_{\rm g}+\phi_{\rm s}\rho_{\rm s}}{\phi_{\rm g}+\phi_{\rm s}},$$
$$\rho_1''=\frac{\phi_{\rm g}\rho_{\rm g}+\phi_{\rm w}\rho_{\rm w}}{\phi_{\rm g}+\phi_{\rm w}}. \tag{C5}$$

Appendix D: Expressions of friction coefficients

The b_{12}, b_{13}, b_{14}, b_{23}, b_{24}, b_{34} refer to the friction coefficients between solid grain and water, solid grain and gas, solid grain and gas hydrate, water and gas, water and gas hydrate, gas and gas hydrate, respectively,

$$b_{12}=\eta_{\rm w}S_{\rm w}^2/(\kappa_{\rm s}\kappa_{\rm rw}),\ \ b_{13}=\eta_{\rm g}S_{\rm g}^2/(\kappa_{\rm s}\kappa_{\rm rg}),$$
$$b_{24}=\eta_{\rm w}S_{\rm w}^2/(\kappa_{\rm h}\kappa_{\rm rw}),\ \ b_{34}=\eta_{\rm g}S_{\rm g}^2/(\kappa_{\rm h}\kappa_{\rm rg}), \tag{D1}$$

where $\eta_{\rm w}$ and $\eta_{\rm g}$ are the water viscosity and gas viscosity, respectively. $\kappa_{\rm s}$ and $\kappa_{\rm h}$ denote the effective permeabilities of the solid grain frame and hydrate frame $\kappa_{\rm s}=\kappa_{\rm s0}\left(\phi_{\rm w}/\phi\right)^3$, $\kappa_{\rm h}=\kappa^{\rm h0}\left(\phi/\phi_{\rm h}\right)^2\left(\phi_{\rm w}/\phi_{\rm s}\right)^3$, where $\kappa_{\rm s0}$ and $\kappa^{\rm h0}$ are permeabilities of the solid grain frame and hydrate frame.

According to the work of Berryman and Wang,[41] the friction coefficient between solid grain and gas hydrate b_{14} is defined as

$$b_{14}=b_{14}^0\left(\phi_{\rm h}(1-\phi)\right)^2, \tag{D2}$$

where the value of the coefficient $b_{14}^0=2.2\times10^8$ is determined, which was suggested by Guerin.[29]

The expression of the friction coefficient between water and gas can follow the work of Santos *et al.*[9] $b_{23}=S_{\rm w}S_{\rm g}k_{\rm rgw}\sqrt{\eta_{\rm g}\eta_{\rm w}}/D$, where $D=\kappa_{\rm s}(k_{\rm rg}k_{\rm rw}-k_{\rm rgw}^2)$, $k_{\rm rgw}=\sqrt{\varepsilon_0 k_{\rm rg}k_{\rm rw}}$, ε_0 is a constant, set to 0.1. $\kappa_{\rm s}$ is the absolute permeability of the porous medium, $\kappa_{\rm rw}$ and $\kappa_{\rm rg}$ are the relative permeability of gas and fluid, respectively, which can be expressed as

$$\kappa_{\rm rg}=(S_{\rm g}-S_{\rm rg})^2(1-S_{\rm rg})^{-2},$$
$$\kappa_{\rm rw}=(S_{\rm w}-S_{\rm rw})^2(1-S_{\rm rw})^{-2}. \tag{D3}$$

Acknowledgment

Project supported by the National Natural Science Foundation of China (Grant Nos. 12304496 and 12334019).

References

[1] Biot M A 1956 *J. Acoust. Soc. Am.* **28** 168
[2] Biot M A 1956 *J. Acoust. Soc. Am.* **28** 179
[3] Biot M A 1962 *J. Appl. Phys.* **33** 1482
[4] Biot M A 1962 *J. Acoust. Soc. Am.* **34** 1254
[5] Plona T J 1980 *Appl. Phys. Lett.* **36** 259
[6] Helgerud M B, Dvorkin J, Nur A M, Sakai A and Collett T 1999 *Geophysical Research Letters* **26** 2021
[7] Ecker C, Dvorkin J and Nur A M 2000 *Geophysics* **65** 565
[8] Santos J E, Douglas Jr J, Corberó J and Lovera O M 1990 *J. Acoust. Soc. Am.* **87** 1439
[9] Santos J E, Ravazzoli C L, Gauzellino P M, Carcione J M and Cavallini F 2004 *Journal of Computational Acoustics* **12** 1
[10] Lo W C, Sposito G and Majer E 2005 *Water Resources Research* **41** W02025
[11] Lo W C, Yeh C L and Lee J W 2015 *Advances in Water Resources* **83** 207
[12] Vasco D W 2013 *Geophysics* **78** L1
[13] Santos J E and Savioli G B 2015 *J. Acoust. Soc. Am.* **138** 3033
[14] Santos J E and Savioli G B 2016 *J. Acoust. Soc. Am.* **139** 693
[15] Leclaire P, Cohen-Tenoudji F and Puente J 1994 *J. Acoust. Soc. Am.* **96** 3753
[16] Carcione J M and Seriani G 2001 *Journal of Computational Physics* **170** 676
[17] Ruppel C D 2007 *Elements* **3** 29
[18] Liu T T, Han L G and Ge Q X 2019 *Waves in Random and Complex Media* **31** 207
[19] Boswell R 2009 *Science* **325** 957
[20] Chong Z R, Yang S H B, Babu P, Ling P and Li X S 2016 *Applied Energy* **162** 1633
[21] Sadeq D, Alef K, Iglauer S, Lebedev M and Barifcani A 2018 *International Journal of Hydrogen Energy* **43** 23193
[22] Yan C L, Cheng Y F and Li M L 2017 *International Journal of Hydrogen Energy* **42** 19810
[23] Wang X J, Wu S G and Liu X W 2006 *Chinese J. Geophys.* **49** 504
[24] Wang X J, Wu S G and Liu X W 2010 *Geoscience* **24** 993
[25] Wang X H, Xu Q, He Y N, Wang Y F, Sun Y F, Sun C Y and Chen G J 2019 *Energies* **12** 1825
[26] Lee M W and Waite W F 2008 *Geochemistry, Geophysics, Geosystems* **9** Q07008
[27] Zhang Y W, Liu X W and Jin Y J 2004 *Oil Geophysical Prospecting* **39** 205
[28] Zhang R W, Li H Q, Wen P F and Zhang B J 2016 *Chinese J. Geophys.* **59** 3417
[29] Guerin G and Goldberg D 2005 *Geochemistry, Geophysics, Geosystems* **6** 1
[30] Liu L, Zhang X and Wang X 2021 *Energies* **14** 804
[31] Liu L, Zhang X and Wang X 2024 *Geophysics* **89**
[32] Zhou Y, Zhang X, Liu L, Liu T and Wang X 2022 *Progress Theoretical and Experimental Physics* 123A01
[33] Liu L, Zhang X and Wang X 2021 *Chin. Phys. B* **30** 024301
[34] Carcione J M, Cavallini F, Santos J E, Ravazzoli C L and Gauzellino P 2004 *Wave Motion* **39** 227
[35] Ba J, Carcione J M and Nie J X 2011 *Journal of Geophysical Research* **116** B06202
[36] Liu T, Liu X and Zhu T 2020 *Marine & Petroleum Geology* **112** 104036
[37] Yang H D, Fu L Y, Fu B Y and Du Q Z 2022 *Geophysics* **87** 329
[38] Huang J D, Yang D H, He X J and Chang Y F 2023 *Geophysics* **88** 121
[39] Wang N X, Du B and Du G 1987 *Well Logging Technology* **11** 26
[40] Xu X K, Chen X L, Fan Y R, Li X, Liu M J and Hu H C 2012 *Journal of China University of Petroleum* **36** 97
[41] Berryman J G and Wang H F 2000 *International Journal of Rock Mechanics & Mining Sciences* **37** 63